High Energy Physics and Nuclear Physics

Vol. 13, No. 4

High Energy Hadrons in Atmospheric Cosmic Rays Observed with Fe Emulsion Chambers

Zhang Naijian, Wang Chengrui, He Mao, Cao Peiyuan, Li Jinyu, Zou Baotang, Wang Guangjun and Wei Chao

(High Energy Physics Group, Shandong University, Jinan)

A part of K4 (1984--1985) Fe emulsion chambers exposed at Mt. Kanbala (altitude 5500 m, atmospheric depth 520 g/cm^2) by China-Japan Emulsion Chamber Collaboration has been analyzed with systematic scanning and measurement. The distribution of the starting depths of the observed showers is given. The zenith angle distribution, vertical intensity, energy spectrum and attenuation length of hadrons in air and in iron are presented. Our results are compared with the recent data given by other experiments, and they are approximately consistent with each other.

1. INTRODUCTION

The hadronic component of atmospheric cosmic rays observed at mountain altitudes carries more directly messages from high energy interactions. Analysis of secondary hadrons produced in cosmic ray high energy nuclear interactions using mountain emulsion chambers can provide cosmic ray morphological data as well as important information about the mechanism of high energy hadronic interaction and the mass spectrum of primary cosmic rays above 10^{15} eV.

In the past few years, Mt. Kanbala Emulsion Chamber Collaboration has published a series of experimental results about the electromagnetic and hadronic components in the atmospheric cosmic rays [1-9]. Other experimental groups, e.g. Fuji Group [10,11], Pamir Group [12, 13], etc.

Supported by the National Natural Science Foundation of China.
Received on January 30, 1989.

reported on the same topic also. While the published experimental data of hadronic components of atmospheric cosmic rays mentioned above were mainly obtained by means of Pb chambers, the results presented in this paper were observed with Fe chambers, which are more efficient in detecting hadrons.

Interactions of high energy hadrons of cosmic rays with Pb or Fe nuclei of the emulsion chambers produce secondary particles, form showers in the chambers and are finally recorded by the photosensitive layers. The mean free path of nuclear interaction of hadrons with Pb is 31 r.l., while that with Fe is 9.4 r.l., hence the detection probability of hadrons in Fe chambers is higher than that in Pb chambers of the same thickness expressed in r.l. As pointed out in Ref.[7], the detection probability for hadrons in Fe emulsion chambers of thickness 28--30 r.l. is twice as large as the corresponding value in Pb chambers. In order to observe the hadron component more efficiently, the China-Japan Emulsion Chamber Collaboration has installed large-area Fe emulsion chambers on Mt. Kanbala (altitude 5500 m, atmospheric depth 520 g/cm^2) since 1982, and some experimental results on the electromagnetic and hadronic components of atmospheric cosmic rays have already been reported in the past few years [5-7].

To investigate the characteristics of high energy hadrons in the atmospheric cosmic rays, we made systematic scanning, measurements and analyses of a portion of the Mt. Kanbala K4 emulsion chambers. The starting point distribution of shower events, the zenith angle distribution, the vertical intensity and the integral energy spectrum of high energy atmospheric hadrons and the attenuation lengths of hadrons in air and Fe are given, with comparisons and discussions in connection with the corresponding results of other groups.

2. EXPERIMENT

The thickness of each block of Mt. Kanbala Fe K4 emulsion chambers is 29 r.l., which is composed of 59 Fe plates with a size of 60 cm × 90 cm × 9 mm, interleaved with 13 layers of vacuum sealed photosensitive materials with an area of 40 cm × 50 cm, beginning from the fifth r.l. The X-ray films used are of Sakura-N type, Fuji-100 type and Tianjin III type (high Ag content). The exposure began from May, 1984 to May, 1985 and the total chamber area was 58 m^2. The experimental data used in this paper were obtained from a portion of it, 7.8 m^2.

The darkness of shower events identified through scanning, angular measurements and target mapping are determined by means of an NLM-C microphotometer with an aperture size of 200 μm × 200 μm. The method of shower energy determination in the Fe chamber is essentially the same as that used in the Pb chamber [7].

The shower events can be classified into γ-ray showers and hadron jets on the basis of the starting depth distribution and the interaction characteristics. Showers starting at depths $\Delta t \leq$ 6 r.l. and without observable subsequent interactions are generally considered as initiated by γ-rays, whereas the remaining ones are classified as hadron jets. In the present experiment, a total number of 405 shower events with $E_h^{(\gamma)} >$ 5 TeV are observed in 39 blocks of Fe chambers, among which the number of non-correlated high energy shower events satisfying $\Delta t >$ 6 r.l. and $E_h^{(\gamma)} \geq$ 7 TeV is 147, where E_h represents the electromagnetic energy transformed from the secondary particles produced in hadron-Fe nucleus interaction. In the data processing, the effective spatial region for recording hadrons was taken as $6 \leq \Delta t \leq$ 23 r.l., and events entering the chamber blocks obliquely without traversing their top surfaces were rejected.

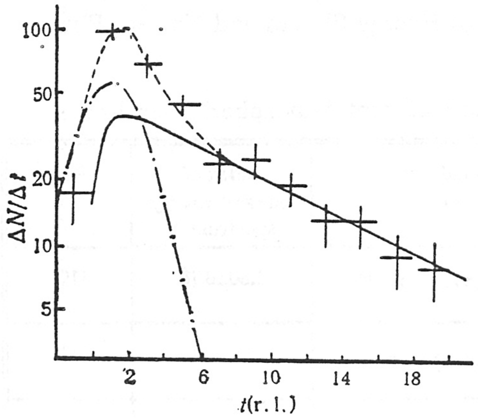

FIG.1

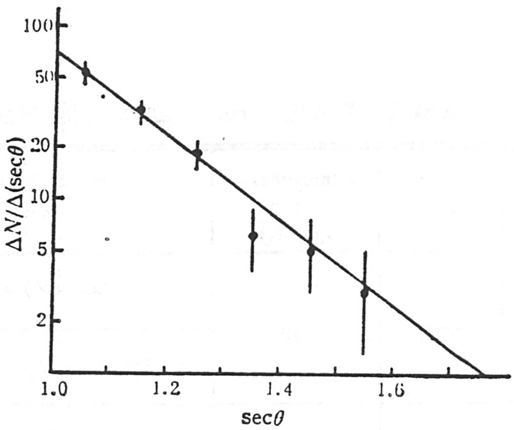

FIG.2

FIG.1 The starting point distribution of shower events. The dotted line is the experimental fit of the distribution of all shower events and the dot-dash line and the solid curve represent the expected distributions of γ-rays and hadrons respectively.

FIG.2 The zenith angle distribution of hadrons.

3. EXPERIMENTAL RESULTS AND DISCUSSIONS

3.1 The Starting Point Distribution of Showers and the Attenuation Length of Hadrons in Fe

The starting point distribution of all shower events observed in the experiment are shown in Fig.1 marked with "+". The dotted curve is the distribution fitting all the experimental points, where the events in the peak region at small depths are due to γ-rays and a portion of hadrons, while those in the deep region (e.g. $\Delta t > 6$ r.l.) are due to hadrons. Expected distributions of γ-rays and hadrons can be obtained by fitting the experimental points in the two regions separately according to the different attenuation lengths of γ-rays and hadrons in Fe.

Based on the slope of the solid curve in Fig.1 at $\Delta t > 6$ r.l., the attenuation length of hadrons in Fe is determined to be $\lambda_{Fe} = 11.2 \pm 1.1$ r.l. This result is roughly consistent with the early Mt. Fuji value [14] $\lambda_{Fe} = 11.5 \pm 1.5$ r.l., the recent Mt. Kanbala (China-Japan Collaboration) data [7] $\lambda_{Fe} = 13.5$ r.l. and the extrapolation of the results given in Ref.[15], i.e. $\lambda_{Fe} = 14.5$ r.l.

3.2 The Zenith Angle Distribution and Attenuation Length of Hadrons in the Atmosphere

The zenith angle distribution of hadrons is shown in Fig.2. The attenuation length of hadrons in air can be obtained by fitting the experimental points which are the ratio of the intensity $J(x, \theta)$ of cosmic ray particles with direction θ to the vertical intensity $J\perp(x)$ at atmospheric depth x. The result is $\lambda = 93 \pm 9$ g/cm^2. This is in agreement with the attenuation lengths of γ-rays and hadrons in air, $\lambda = 95$ g/cm^2, recently summarized [16].

3.3 The Integral Energy Spectrum and Vertical Intensity of Hadrons

The integral energy spectrum of hadrons is shown in Fig.3, which is of exponential form. The index of the exponential energy spectrum fitted with the experimental points (in $E_h^{(\gamma)} \geq 10$ TeV region) is $\beta = 1.85 \pm 0.18$.

TABLE 1 The Experimental Data for Hadrons at Different Atmospheric Depths

Site of obs.	Altitude (m)	Atmospheric depth (g/cm$_2$)	Vertical intensity of Hadrons $J_\perp(\mathrm{cm}^{-2}\cdot\mathrm{s}^{-1}\cdot\mathrm{sr}^{-1})$	Index of integral energy spectrum β	Ref.
Mt. Fuji	3776	650	$J_\perp(E_h^{(\gamma)}\geqslant 5\mathrm{TeV}) = (1.5\pm0.1)\times10^{-10}$	1.80±0.18	[10]
			$J_\perp(E_h^{(\gamma)}\geqslant 5\mathrm{TeV}) = (2.1\pm0.1)\times10^{-10}$	2.0±0.1	[11]
Pamir	4370	596	$J_\perp(E_h^{(\gamma)}\geqslant 5.5\mathrm{TeV}) = (1.6\pm0.1)\times10^{-10}$	2.04±0.07	[12]
			$J_\perp(E_h^{(\gamma)}\geqslant 5\mathrm{TeV}) = (2.7\pm0.1)\times10^{-10}$	1.9±0.1	[13]
Mt. Kanbala	5500	520	$J_\perp(E_h^{(\gamma)}\geqslant 5\mathrm{TeV}) = (6.0\pm0.6)\times10^{-10}$	2.03±0.08	[5]
			$J_\perp(E_h^{(\gamma)}\geqslant 10\mathrm{TeV}) = (1.4\pm0.2)\times10^{-10}$	1.90±0.10	[7]
			$J_\perp(E_h^{(\gamma)}\geqslant 10\mathrm{TeV}) = (1.6\pm0.2)\times10^{-10}$	1.85±0.18	This work

Due to the higher detection threshold energy of the Fe emulsion chamber, the detection efficiency in the low energy part of the energy spectrum is correspondingly poorer. But for high energy hadrons with $E_h^{(\gamma)}\geq 10$ TeV, such detection bias does not exist.

Let S be the area of the emulsion chamber, T the exposure time, P the detection probability for hadrons and Ω the effective solid angle of the emulsion chamber for hadrons, then the relationship between the vertical intensity of hadrons $J\perp(\geq E_h^{(\gamma)})$ and the experimentally observed number of hadrons $N_{obs}(\geq E_h^{(\gamma)})$ will be $J\perp(\geq E_h^{(\gamma)}) = N_{obs}(\geq E_h^{(\gamma)})/(S{\cdot}T{\cdot}P{\cdot}\Omega)$.
Under present experimental conditions, the product of the hadron detection probability and the effective solid angle of the chamber is $P{\cdot}\Omega \approx 0.23$ sr [9]. From the calculations based on the experimental data, we finally obtain the vertical intensity of atmospheric cosmic ray hadrons in the energy range $10 \leq E_h^{(\gamma)} \leq 100$ TeV, at the altitude of Mt. Kanbala

$$J_\perp(\geqslant E_h^{(\gamma)}) = (1.6\pm0.2)\times 10^{-10}\left(\frac{E_h^{(\gamma)}}{10}\right)^{-(1.85\pm0.18)}\ \mathrm{cm}^{-2}\cdot\mathrm{s}^{-1}\cdot\mathrm{sr}^{-1}.$$

3.4 Variation of Vertical Intensity of Hadrons With Atmospheric Depth

The vertical intensities and the indices of the integral energy spectrum of atmospheric cosmic ray hadrons reported in recent years by the Mt. Fuji Group, the Pamir Group and the Mt. Kanbala Group are compiled in Table 1. It can be seen from the table that the indices of the energy spectrum of hadrons given by these groups are close to each other. On the other hand, comparing the vertical intensities of hadrons published by these groups in different periods as listed in Table.1, it can be seen that the recent data given by Fuji and Pamir [11,13] are about 40% higher than the corresponding earlier ones (reduced values in the same energy range) [10,12]. In contrast to the old results, the new energy spectra of hadrons and γ-rays move toward the high energy side, whereas the spectral indices remain practically unchanged and thus result in higher intensities [17].

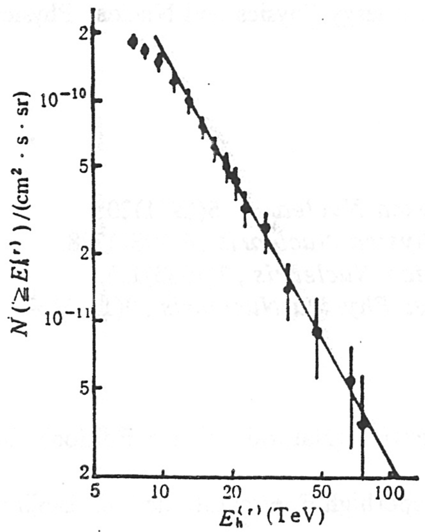

FIG.3

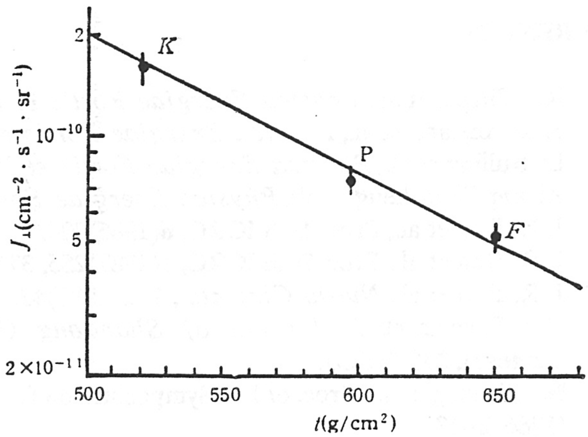

FIG.4

FIG.3 The vertical integral energy spectrum of hadrons.

FIG.4 The vertical intensities of cosmic ray hadrons at different atmospheric depths (— $\geq$ 10 TeV): K–Kanbala (the present work), P–Pamir[13] and F–Fuji[11].

Reducing all the vertical intensities of the atmospheric cosmic ray hadrons given by Fuji [11] and Pamir [13] and that observed with Fe emulsion chambers in the present work in the same energy range ($E_h^{(\gamma)} \geq 10$ TeV) and plotting the results vs. the atmospheric depth, the results are shown in Fig.4, where the solid line is the fit of experimental points, taking the attenuation length of hadrons in air to be $\lambda = 100\ g/cm^2$. It can be seen that the solid line is consistent with the experimental points.

4. CONCLUDING REMARKS

The present work has shown that the attenuation length in the atmosphere, the vertical intensity and the integral energy spectrum of high energy hadrons observed by Fe emulsion chambers are in agreement with those obtained by Pb emulsion chambers, and also that the attenuation length of hadrons in iron is consistent with the results given by other experiments. The above results provide further experimental data for the characteristics of high energy hadrons ($E_h^{(\gamma)} \geq$ 10 TeV) of atmospheric cosmic rays at the altitude of Mt. Kanbala using Fe emulsion chambers, and yield various morphological results when compared with those obtained by Pb emulsion chambers.

ACKNOWLEDGEMENT

The authors would like to express their thanks to the colleagues of the Mt. Kanbala Emulsion Chamber Collaboration for their support and their enormous amount of experimental work. We are also grateful to Prof. J. R. Ren of IHEP, Chinese Academy of Sciences, for his help and useful discussions.

REFERENCES

[1] Ren Jingru et al., *Physica Energiae Fortis et Physica Nuclearis* , **5**(1981)205.
[2] Huo Anxiang et al., *Physica Energiae Fortis et Physica Nuclearis* , **6**(1982)778.
[3] Lu Suiling et al., *Physica Energiae Fortis et Physica Nuclearis* , **7**(1983)118.
[4] Zhang Chunsheng et al., *Physica Energiae Fortis et Physica Nuclearis* , **9**(1985)649.
[5] J. R. Ren et al., Proc. 19th ICRC, **6**(1985)204.
[6] J. R. Ren et al., Proc. 20th ICRC, **5**(1987)255, 371.
[7] J. R. Ren et al., *Nuovo Cimento* , **10C**(1987)43.
[8] Cao Peiyuan et al., *Journal of Shandong University* (Natural Science Edition) (in Chinese), **23**(1988)31.
[9] N. J. Zhang et al., Proc. of Int. Symposium on C. R. Superhigh Energy Interactions, Beijing (1986)2--13.
[10] M. Akashi et al., Proc. 17th ICRC, **5**(1981)247.
[11] M. Amenomori et al., Proc. 19th ICRC, **6**(1985)208.
[12] S. G. Bayburina et al, Proc. 18th ICRC, **5**(1983)420.
[13] S. D. Cananov et al., Proc. 19th ICRC, **6**(1985)216.
[14] M. Shibata et al., *Nuovo Cimento* , **39B**(1977)302.
[15] Berkely Particle Data Group, Particle Properties Data Booklet (1986), p.162.
[16] E. H. Shibuya, Proc. 20th ICRC, **8**(1987)238.
[17] Zhang Naijian et al., *Journal of Shandong University* (Natural science Edition) (in Chinese), **22**(1987)69.